ACS Photonics

Letter

Cite This: ACS Photonics 2020, 7, 43−48

pubs.acs.org/journal/apchd5

Modifying the Spectral Weights of Vibronic Transitions via Strong Coupling to Surface Plasmons

Rahul Deshmukh,[†,‡] Paulo Marques, Anurag Panda,[§] Matthew Y. Sfeir,[‡,∥] Stephen R. Forrest,*[,§,⊥] and Vinod M. Menon*[,†,‡]

[†]Department of Physics, City College of the City University of New York (CUNY), New York, New York 10031, United States
[‡]Department of Physics, Graduate Center of the City University of New York (CUNY), New York, New York 10016, United States
[§]Department of Materials Science and Engineering, University of Michigan, Ann Arbor, Michigan 48109, United States
[∥]Photonics Initiative, Advanced Science Research Center, City University of New York, New York, New York 10031, United States
[⊥]Department of Electrical Engineering and Computer Science and Physics, University of Michigan, Ann Arbor, Michigan 48109, United States

Supporting Information

ABSTRACT: Strong light−matter coupling results in the formation of hybrid half-light half-matter excitations with modified energy levels. The strong coupling of excitons with photons in organic molecular systems has received much attention recently owing to the potential for engineering their photophysical properties and even the prospects for controlling chemical reactions. One means to affect chemical reactions is to control the molecular excited states within their vibronic manifolds. Here we demonstrate the modification of the spectral weight of the vibronic transitions and excimer emission in an archetype organic molecule, diindenoperylene (DIP), by strong coupling to surface-plasmon polaritons. The vertically aligned DIP molecule is grown on an ultrasmooth film of Ag with a 3 nm thick alumina spacer. Through angle-resolved reflectivity measurements we demonstrate the strong coupling between the surface-plasmon mode of the Ag and the vibronic transitions in DIP. Temperature-dependent photoluminescence measurements show the shift in the spectral weight of the emission peaks when the molecules are in the strong coupling regime—changes that are attributed to the polaritonic control of the oscillator strengths of emissive states owing to modification in the Franck−Condon factor and efficient energy transfer to lower-lying excimer states. This work demonstrates the potential to modify the material properties through a strong light−matter interaction.

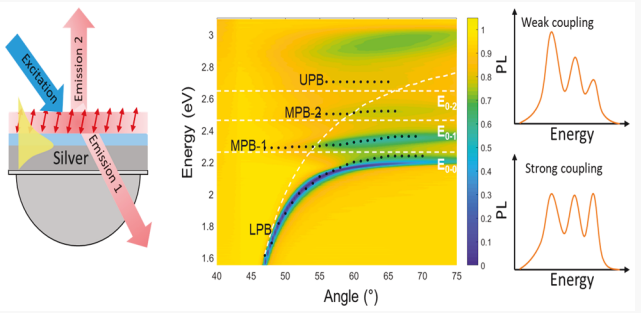

KEYWORDS: *strong coupling, surface plasmons, vibronic transitions, diindenoperylene, photoluminescence, energy transfer*

Strong exciton−photon coupling resulting in the formation of half-light/half-matter quasiparticles, termed exciton polaritons, has been explored in a variety of material systems ranging from inorganic quantum wells to organic molecular systems and, more recently, in 2D semiconductors.[1−3] Several fundamental and technologically relevant phenomena ranging from condensation to polaritonic circuits have been uncovered in coupled light−matter systems.[4] More recently, strong coupling in organic molecular systems has received interest following the realization of polariton lasing, Bose−Einstein condensation, and even superfluidity at room temperature.[5−8] Whereas these demonstrations exploited the more conventional polaritonic phenomena, there has also been consideration of altering chemical reaction pathways via strong coupling to both electronic transitions and infrared vibrational modes.[9−12] Indeed, this latter theme has opened up the question of "materials engineering" within optical cavities.[13−15] Organic molecular solids are characterized by well resolved vibronic transitions in their absorption and emission spectra that can be hybridized with photons in optical microcavities.[16,17] There have also been theoretical predictions on the novel effects on vibronic decoupling and an increase in coherence under strong light−matter coupling.[18] Following this line of investigation, here we demonstrate the modification of the relative weights of spectral features arising from vibronic transitions in an archetype organic molecule, diindenoperylene (DIP), when it is strongly coupled to surface plasmons of a Ag film. Because vibronic modes are linked to the reactive properties of organics, the control of the energetic landscape of excited states ultimately may lead to changes in molecular reaction kinetics. Unlike conventional microcavities, the use of plasmons in planar films and lattices has received interest owing to the simplicity of the structure, the possibility of

Received: September 20, 2019
Published: December 26, 2019

DOI: 10.1021/acsphotonics.9b01357
ACS Photonics 2020, 7, 43−48

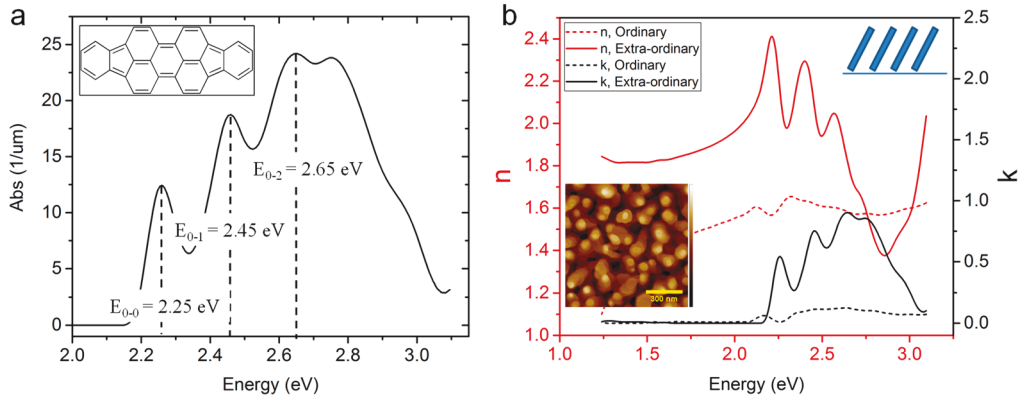

Figure 1. (a) Absorption spectrum of DIP. Also shown are the specific vibronic transitions of interest. The inset shows the molecular structure. (b) Ellipsometric data showing the ordinary and extraordinary refractive index (real and imaginary parts) for the upstanding DIP film. (Inset) Surface profile obtained by atomic force microscopy (max height = 40 nm, scale bar = 300 nm). The refractive index of the flat-lying film along with the AFM image is shown in Figure S1.

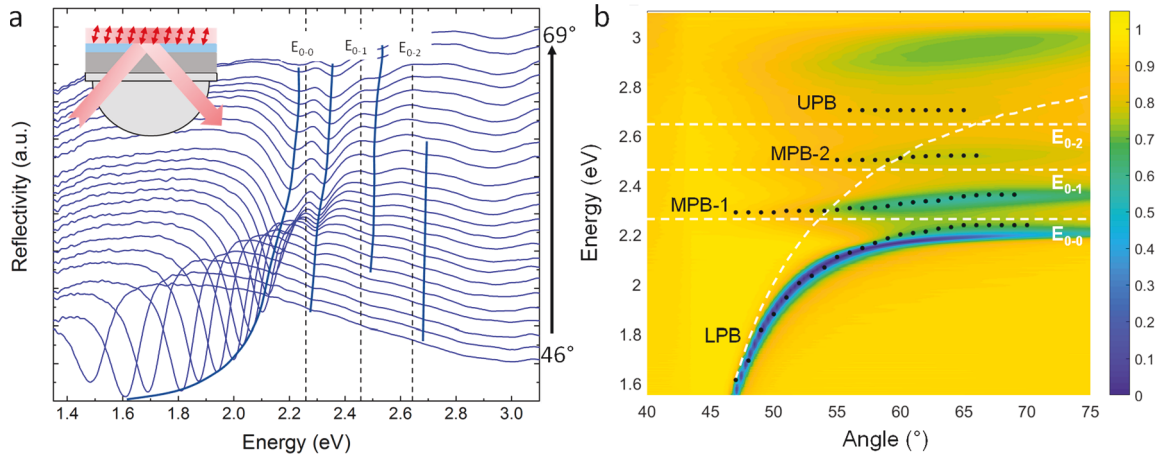

Figure 2. (a) Angle-resolved reflectivity spectra for DIP on silver. The inset shows the Kretschmann geometry used here. Details of the layers at the bottom. (b) Simulated (color plot) and experimental (black dots) data from the reflectivity experiment. The horizontal white dashes show the vibronic transitions E_{0-0}, E_{0-1}, and E_{0-2}. The dashed white curve shows the original surface-plasmon dispersion for bare silver adjusted for a pure dielectric spacer of the same thickness as DIP.

engineering the dispersion in a straightforward manner, and the comparatively small volume occupied by the electromagnetic modes.[19−25]

The samples consist of 50 nm thick, ultrasmooth Ag films deposited via vacuum thermal evaporation in a system (base pressure of 10^{-7} Torr) on glass coverslips precoated with a 2 nm thick Ge wetting layer.[26] This was followed by the deposition of 35 nm of DIP on a 3 nm Al_2O_3 layer that minimizes the oxidation of Ag while also separating the molecules from direct contact with the metal film to avoid nonradiative polariton quenching. The deposition rate of 3 Å/s was chosen to achieve vertically oriented molecules so that the dipole efficiently couples to the Ag surface plasmons.

The chemical structure of DIP along with its room-temperature optical absorption spectrum is shown in Figure 1a. The absorption spectrum exhibits multiple peaks separated by equal energy intervals that correspond to the E_{0-0}, E_{0-1}, and E_{0-2} vibronic transitions at 2.25, 2.45, and 2.65 eV, respectively. The additional maximum at 2.75 eV originates from the Davydov splitting arising in monoclinic DIP crystals with a basis of two. The orientation of the molecules was established via ellipsometry and atomic force microscopy (AFM). The ellipsometry data showing the ordinary and extraordinary refractive index are plotted in Figure 1b. The imaginary component of the extraordinary refractive index shows significantly stronger absorption peaks as compared with the ordinary refractive index. Because absorption is higher along the stacking direction, this suggests that the DIP molecular planes are vertically oriented relative to the substrate.[27,28] The inset of Figure 1b also shows an AFM image of the film. Protrusions with diameters ranging from 50 to 100 nm in diameter are observed, suggesting a strained-layer, Stranski−Krastanov growth mode. Additional information about the sample fabrication and growth can be found in the Supporting Information. Also shown in Figure S1 are the ellipsometry data for the flat-lying DIP film along with its AFM image. In this case, the extraordinary index is lower than that of the ordinary axis, from which we infer the molecules now lie flat relative to the substrate. Indeed, the flat orientation is supported by the nanocrystalline surface morphology where the protrusions (AFM image) in Figure 1b are now tightly clustered and apparently relaxed and lying parallel to the substrate.

The glass substrate allows for angle-resolved reflectivity experiments performed in the Kretschmann configuration shown in the inset of Figure 2a to enable coupling of surface

DOI: 10.1021/acsphotonics.9b01357
ACS Photonics 2020, 7, 43−48

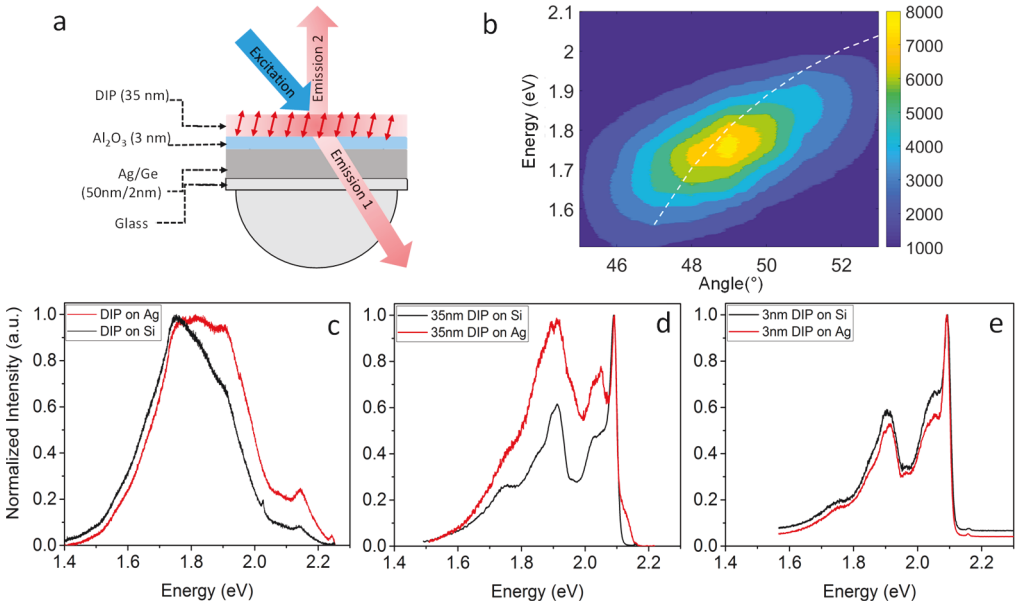

Figure 3. (a) Two configurations used for the photoluminescence (PL) experiments. (b) Color plot showing PL spectra obtained from Emission 1. The white dashed line shows a lower polariton branch from Figure 2b. (c) PL spectra (Emission 2) obtained from the DIP on silver and the control sample (DIP on silicon) at room temperature. PL spectra (Emission 2) at 70 K from (d) 35 nm DIP on silver and silicon and (e) 3 nm DIP on silver and silicon. The 35 nm DIP is in the strong coupling regime, whereas the 3 nm DIP is in the weak coupling regime and shows emission spectra very similar to those of the control sample on silicon.

plasmons to the vibronic transitions in DIP. Tracing the dips in the reflectivity spectra shown in Figure 2a versus the angle reveal the dispersion of the strongly coupled surface-plasmon–exciton hybrid modes. Figure 2b shows the experimental data (black dots) overlaid on transfer matrix simulations of the coupled system. The color plot shows the simulated reflectivity, with the dark areas corresponding to the reflectivity minima. Agreement between the measured and calculated spectral shapes as well as the anticrossing energies is observed by assuming a DIP thickness of 21 nm, as opposed to the deposited thickness of 35 nm. We attribute this discrepancy to the nonuniformities in the deposition that lead to a fraction of molecules not oriented precisely normal to the film surface. This variation in the dipole orientation reduces the "effective thickness" of the DIP layer that can be coupled to surface plasmons. The different experimentally observed plasmon–exciton hybrid states are identified as the lower polariton branch (LPB), middle polariton branches 1 and 2 (MPB-1 and MPB-2), and the upper polariton branch (UPB). These branches show avoided crossings at the energies corresponding to the vibronic transitions of DIP, leading to Rabi splitting energies of 95 meV between LPB and MPB-1, 131 meV between MPB-1 and MPB-2, and 190 meV between MPB-2 and UPB.

Taking into account the three vibronic transitions of DIP and the one surface-plasmon mode, we use a 4 × 4 Hamiltonian to obtain the Hopfield coefficients (Figure S2) that gives the relative contribution of each oscillator in the various polariton branches. The hybridization between the vibronic transitions and the surface plasmon plays a central role in the modification of weights of individual spectral features in the polaritonic emission.

We employed two different experimental configurations to obtain the steady-state photoluminescence (PL) of the samples. As shown in Figure 3a, the setups are similar to the experiments by Bellessa et al.[19] and Symonds et al.[29] In the first case, the sample is illuminated via the DIP film, and the angle-dependent transverse magnetic (TM) PL emission is collected through the underlying Ag using a prism and a polarizer (Emission 1). The PL spectrum is shown in Figure 3b, where the Stokes-shifted emission peak follows the dispersion of the lower polariton branch. The intensity of the emission is maximum at a 49° collection angle, corresponding to the resonance with the lower polariton branch, and decreases rapidly for larger and smaller angles. This is in agreement with a recent theoretical prediction for enhanced PL at the crossover point in the strong coupling regime.[30] In the second case, the reflected PL (Emission 2) was collected to understand the modification in the emission properties without being filtered through surface-plasmon modes. Similar experiments were performed on a 35 nm thick DIP film on a Si substrate (the "control"). The PL spectra obtained from the DIP on Ag at room and low temperature (70 K), along with the PL from a control, are shown in Figure 3c,d, respectively. The PL from thin films of DIP has been known to exhibit complex emission profiles including strong, featureless, and red-shifted excimer emission at room temperature.[31,32] We find similar emission spectra on the control thin film. However, the strongly coupled sample exhibits spectrally broader emission. The modification in the PL spectrum is more distinct at lower temperatures where the strength of the excimer emission (E–0) is similar to the highest oscillator strength emission line (0–0) in the strongly coupled sample. (See Figure 3d.)

Similar experiments were carried out for samples with 3 nm thick DIP on both Si and Ag. Angle-resolved reflectivities did not exhibit the anticrossing seen in the thicker samples, indicative of only weak coupling. (See Figure S3.) The emission spectra from the weakly coupled samples (Figure 3e) show no difference between the control and the Ag film samples. This indicates that the spectral redistribution observed in the 35 nm thick DIP sample on Ag is indeed

DOI: 10.1021/acsphotonics.9b01357
ACS Photonics 2020, 7, 43–48

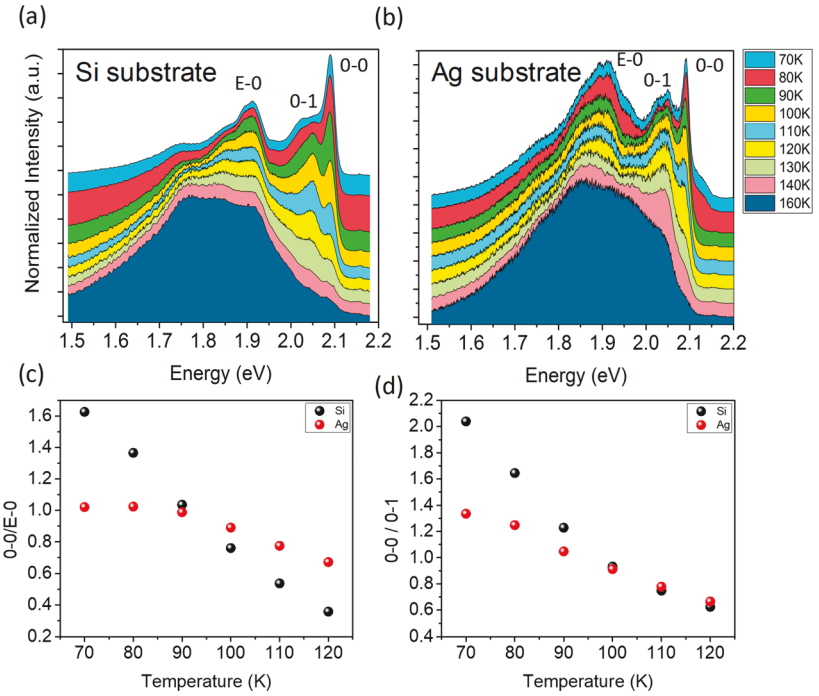

Figure 4. Temperature evolution of PL spectra (Emission 2) from (a) a control sample of DIP on the Si substrate and (b) DIP on silver. The DIP on silver shows the markedly different evolution of the PL spectra as a function of temperature with the highest oscillator strength transition showing similar intensities as the lower energy transitions. (c) Ratio of the highest oscillator strength transition (0−0) and the excimer transition (E−0) and (d) ratio of the 0−0 transition to the vibronic transition (0−1) showing markedly different temperature evolution under the strong coupling regime owing to the efficient energy transfer to the lower energy excimer transitions and modified oscillator strengths of vibronic transitions owing to the hybridization with the plasmonic mode.

the result of strong coupling. This result differs from previous reports[19,29] on emission from molecules strongly coupled to surface plasmons. There, the PL emission was observed to be either slightly red-shifted[19] or the same as the emission from uncoupled molecules.[29]

The normalized spectrum of the strongly coupled sample shows almost equal emission intensities from the excimer and the vibronic transition peaks, whereas the control has its highest emission at 2.1 eV. This striking modification of the PL spectrum is due to the hybridization of the different vibronic transitions via strong coupling to surface plasmons and the efficient energy transfer to the excimer state. In Figure 4, the PL emission spectra from both the control and the strongly coupled sample are plotted versus the temperature. The three highest energy peaks in the control PL are at 2.09, 2.05, and 1.91 eV and correspond to the 0−0, 0−1, and E−0 transitions, respectively. These peaks are identified as the highest oscillator strength zero-phonon transition (0−0), the lower energy vibronic transition (0−1), and the excimer emission (E−0).

The intensity ratios at these energies, 0−0/E−0 and 0−0/0−1, are plotted in Figure 4c,d for both the strongly coupled (Ag) and control (Si) samples as a function of temperature. From Figure 4c, one see that the ratio of 0−0/E−0 for the control is 1.6 at 70 K and decreases to 0.35 by 120 K. In contrast, the same ratio at 70 K for the strongly coupled sample is ∼1 and remains constant down to T = 100 K, decreasing to 0.7 by 120 K. This observation is indicative of efficient energy transfer from the excited state to the lower energy excimer state under the strong coupling regime. The hybridization with the delocalized plasmonic mode in the strong coupling regime facilitates efficient long-range energy transfer, as has been previously shown in both plasmonic and photonic cavities.[33−36] The same effect is in play here, causing the excited-state population to efficiently transfer energy to the lower-lying excimer states, and hence we see the strength of the 0−0 transition to be comparable to the excimer emission (E−0).

Shown in Figure 4d is the ratio of the 0−0 transition to the lower energy vibronic transit 0−1 arising from the same excited-state manifold. At 70 K, this ratio is ∼2 for the control sample, whereas for the strongly coupled sample it is ∼1.3, indicative of similar oscillator strengths for the 0−0 and 0−1 transitions for the latter case. This modification in the oscillator strength is observed up to 100 K. A plausible explanation for this modification in oscillator strength is the hybridization of the excited-state manifold, with the plasmonic modes resulting in transformed excited-state potentials resulting in a reduced Franck−Condon factor.[37] Furthermore, the lifetimes of the main transition and the vibronic transitions are also modified due to the strong coupling to the surface plasmons.[38]

In summary, strong coupling between surface plasmons on a 50 nm thick Ag film and multiple vibronic transitions in the small-molecular-weight material, DIP, are demonstrated. PL arising from the strongly coupled DIP on Ag shows a redistribution of the spectral weights as compared with the control samples on Si substrates. This spectral redistribution results in a modification of the contributions from the individual vibronics and excimer states in DIP over a temperature range from 70 to 300 K. Similar experiments performed with a thinner DIP film on Ag in the weak coupling regime show no spectral differences with respect to a similar film on Si. The observed modification in the spectral weights under strong coupling to surface plasmons results from the

DOI: 10.1021/acsphotonics.9b01357
ACS Photonics 2020, 7, 43−48

hybridization of the multiple vibronic modes and thus the mixing of the oscillator strengths of the transitions and the efficient energy transfer from the highest oscillator transitions (0−0) to the excimer states (E−0). In addition, the reduced mass of the strongly coupled state alters the curvature of the singlet exciton manifold, thereby modifying the vibronics and leading to clearly distinct changes in the transition spectra. These demonstrations suggest a pathway to controlling the emission spectra of molecules via modifications of their vibronic transitions. They also suggest a need for an improved understanding of the role of strong coupling in the dynamics of the PL properties of molecular materials.

■ ASSOCIATED CONTENT

Supporting Information

The Supporting Information is available free of charge at https://pubs.acs.org/doi/10.1021/acsphotonics.9b01357.

Additional details of sample fabrication, optical properties and fabrication of flat-lying (horizontal orientation) DIP, theoretical model for Hopfield coefficients, simulation results, and angle-resolved reflectivity data for weak coupling of DIP with surface-plasmon polaritons (PDF)

■ AUTHOR INFORMATION

Corresponding Authors

*E-mail: stevefor@umich.edu (S.R.F.).
*E-mail: vmenon@ccny.cuny.edu (V.M.M.).

ORCID

Stephen R. Forrest: 0000-0003-0131-1903
Vinod M. Menon: 0000-0002-9725-6445

Notes

The authors declare no competing financial interest.

■ ACKNOWLEDGMENTS

This work was supported through NSF collaborative grants (DMR 1709996 @ CUNY and DMR1709163 @ the University of Michigan) and the U.S. Department of Energy, Office of Basic Energy Sciences − Physical Behavior of Materials program awards (DE-SC0017760 @CUNY and DE-SC0017971 @ the University of Michigan). We acknowledge useful discussions with Professor Francisco Garcia Vidal.

■ REFERENCES

(1) Weisbuch, C.; Nishioka, M.; Ishikawa, A.; Arakawa, Y. Observation of the Coupled Exciton-Photon Mode Splitting in a Semiconductor Quantum Microcavity. *Phys. Rev. Lett.* **1992**, *69* (23), 3314−3317.

(2) Lidzey, D. G.; Bradley, D. D. C.; Armitage, A.; Walker, S.; Skolnick, M. S. Photon-Mediated Hybridization of Frenkel Excitons in Organic Semiconductor Microcavities. *Science* **2000**, *288* (June), 1620−1624.

(3) Liu, X.; Galfsky, T.; Sun, Z.; Xia, F.; Lin, E.; Lee, Y.-H.; Kéna-Cohen, S.; Menon, V. M. Strong Light−Matter Coupling in Two-Dimensional Atomic Crystals. *Nat. Photonics* **2015**, *9* (1), 30−34.

(4) Sanvitto, D.; Kéna-Cohen, S. The Road towards Polaritonic Devices. *Nat. Mater.* **2016**, *15* (10), 1061−1073.

(5) Kéna-Cohen, S.; Forrest, S. R. Room-Temperature Polariton Lasing in an Organic Single-Crystal Microcavity. *Nat. Photonics* **2010**, *4* (April), 371−375.

(6) Daskalakis, K. S.; Maier, S. A.; Murray, R.; Kéna-Cohen, S. Nonlinear Interactions in an Organic Polariton Condensate. *Nat. Mater.* **2014**, *13* (3), 271−278.

(7) Plumhof, J. D.; Stöferle, T.; Mai, L.; Scherf, U.; Mahrt, R. F. Room-Temperature Bose−Einstein Condensation of Cavity Exciton−Polaritons in a Polymer. *Nat. Mater.* **2014**, *13* (3), 247−252.

(8) Lerario, G.; Fieramosca, A.; Barachati, F.; Ballarini, D.; Daskalakis, K. S.; Dominici, L.; De Giorgi, M.; Maier, S. A.; Gigli, G.; Kéna-Cohen, S.; et al. Room-Temperature Superfluidity in a Polariton Condensate. *Nat. Phys.* **2017**, *13* (9), 837−841.

(9) Thomas, A.; Lethuillier-Karl, L.; Nagarajan, K.; Vergauwe, R. M. A.; George, J.; Chervy, T.; Shalabney, A.; Devaux, E.; Genet, C.; Moran, J.; et al. Tilting a Ground-State Reactivity Landscape by Vibrational Strong Coupling. *Science (Washington, DC, U. S.)* **2019**, *363* (6427), 615−619.

(10) Hutchison, J. A.; Schwartz, T.; Genet, C.; Devaux, E.; Ebbesen, T. W. Modifying Chemical Landscapes by Coupling to Vacuum Fields. *Angew. Chem., Int. Ed.* **2012**, *51* (7), 1592−1596.

(11) Ebbesen, T. W. Hybrid Light-Matter States in a Molecular and Material Science Perspective. *Acc. Chem. Res.* **2016**, *49* (11), 2403−2412.

(12) Muallem, M.; Palatnik, A.; Nessim, G. D.; Tischler, Y. R. Strong Light-Matter Coupling and Hybridization of Molecular Vibrations in a Low-Loss Infrared Microcavity. *J. Phys. Chem. Lett.* **2016**, *7* (11), 2002−2008.

(13) Galego, J.; Garcia-Vidal, F. J.; Feist, J. Cavity-Induced Modifications of Molecular Structure in the Strong-Coupling Regime. *Phys. Rev. X* **2015**, *5* (4), 041022.

(14) Ribeiro, R. F.; Martínez-Martínez, L. A.; Du, M.; Campos-Gonzalez-Angulo, J.; Yuen-Zhou, J. Polariton Chemistry: Controlling Molecular Dynamics with Optical Cavities. *Chem. Sci.* **2018**, *9*, 6325.

(15) Herrera, F.; Spano, F. C. Cavity-Controlled Chemistry in Molecular Ensembles. *Phys. Rev. Lett.* **2016**, *116* (23), 238301.

(16) Holmes, R. J.; Forrest, S. R. Strong Exciton-Photon Coupling and Exciton Hybridization in a Thermally Evaporated Polycrystalline Film of an Organic Small Molecule. *Phys. Rev. Lett.* **2004**, *93* (18), 186404.

(17) Kéna-Cohen, S.; Forrest, S. R. Giant Davydov Splitting of the Lower Polariton Branch in a Polyerystalline Tetracene Microcavity. *Phys. Rev. B: Condens. Matter Mater. Phys.* **2008**, *77*, 073205.

(18) Spano, F. C. Optical Microcavities Enhance the Exciton Coherence Length and Eliminate Vibronic Coupling in J-Aggregates. *J. Chem. Phys.* **2015**, *142* (18), 184707.

(19) Bellessa, J.; Bonnand, C.; Plenet, J. C.; Mugnier, J. Strong Coupling between Surface Plasmons and Excitons in an Organic Semiconductor. *Phys. Rev. Lett.* **2004**, *93* (3), 036404.

(20) Vecchi, G.; Giannini, V.; Gómez Rivas, J. Shaping the Fluorescent Emission by Lattice Resonances in Plasmonic Crystals of Nanoantennas. *Phys. Rev. Lett.* **2009**, *102* (14), 146807.

(21) Törmä, P.; Barnes, W. L. Strong Coupling between Surface Plasmon Polaritons and Emitters: A Review. *Rep. Prog. Phys.* **2015**, *78* (1), 013901.

(22) Chikkaraddy, R.; de Nijs, B.; Benz, F.; Barrow, S. J.; Scherman, O. A.; Rosta, E.; Demetriadou, A.; Fox, P.; Hess, O.; Baumberg, J. J. Single-Molecule Strong Coupling at Room Temperature in Plasmonic Nanocavities. *Nature* **2016**, *535* (7610), 127−130.

(23) Zengin, G.; Wersäll, M.; Nilsson, S.; Antosiewicz, T. J.; Käll, M.; Shegai, T. Realizing Strong Light-Matter Interactions between Single-Nanoparticle Plasmons and Molecular Excitons at Ambient Conditions. *Phys. Rev. Lett.* **2015**, *114* (15), No. 157401.

(24) Zhou, W.; Dridi, M.; Suh, J. Y.; Kim, C. H.; Co, D. T.; Wasielewski, M. R.; Schatz, G. C.; Odom, T. W. Lasing Action in Strongly Coupled Plasmonic Nanocavity Arrays. *Nat. Nanotechnol.* **2013**, *8* (7), 506−511.

(25) Tumkur, T. U.; Zhu, G.; Noginov, M. A. Strong Coupling of Surface Plasmon Polaritons and Ensembles of Dye Molecules. *Opt. Express* **2016**, *24* (4), 3921.

(26) Chen, W.; Thoreson, M. D.; Ishii, S.; Kildishev, A. V.; Shalaev, V. M. Ultra-Thin Ultra-Smooth and Low-Loss Silver Films on a Germanium Wetting Layer. *Opt. Express* **2010**, *18* (5), 5124−5134.

(27) Yokoyama, D.; Sasabe, H.; Furukawa, Y.; Adachi, C.; Kido, J. Molecular Stacking Induced by Intermolecular C − H ··· N Hydrogen

DOI: 10.1021/acsphotonics.9b01357
ACS Photonics 2020, 7, 43−48

Bonds Leading to High Carrier Mobility in Vacuum-Deposited Organic Films. *Adv. Funct. Mater.* **2011**, *21*, 1375−1382.
(28) Yokoyama, D.; Qiang Wang, Z.; Pu, Y.; Kobayashi, K.; Kido, J.; Hong, Z. Solar Energy Materials & Solar Cells High-Efficiency Simple Planar Heterojunction Organic Thin-Film Photovoltaics with Horizontally Oriented Amorphous Donors. *Sol. Energy Mater. Sol. Cells* **2012**, *98*, 472−475.
(29) Symonds, C.; Bonnand, C.; Plenet, J. C.; Bréhier, a.; Parashkov, R.; Lauret, J. S.; Deleporte, E.; Bellessa, J. Particularities of Surface Plasmon−Exciton Strong Coupling with Large Rabi Splitting. *New J. Phys.* **2008**, *10* (6), 065017.
(30) Yuen-Zhou, J.; Saikin, S. K.; Menon, V. Molecular Emission near Metal Interfaces: The Polaritonic Regime. *J. Phys. Chem. Lett.* **2018**, *9* (22), 6511−6516.
(31) Heilig, M.; Domhan, M.; Port, H. Optical Properties and Morphology of Thin Diindenoperylene Films. *J. Lumin.* **2004**, *110* (4), 290−295.
(32) Nichols, V. M.; Broch, K.; Schreiber, F.; Bardeen, C. J. Excited-State Dynamics of Diindenoperylene in Liquid Solution and in Solid Films. *J. Phys. Chem. C* **2015**, *119* (23), 12856−12864.
(33) Coles, D. M.; Somaschi, N.; Michetti, P.; Clark, C.; Lagoudakis, P. G.; Savvidis, P. G.; Lidzey, D. G. Polariton-Mediated Energy Transfer between Organic Dyes in a Strongly Coupled Optical Microcavity. *Nat. Mater.* **2014**, *13* (7), 712−719.
(34) Aberra Guebrou, S.; Symonds, C.; Homeyer, E.; Plenet, J. C.; Gartstein, Y. N.; Agranovich, V. M.; Bellessa, J. Coherent Emission from a Disordered Organic Semiconductor Induced by Strong Coupling with Surface Plasmons. *Phys. Rev. Lett.* **2012**, *108* (6), 066401.
(35) Zhong, X.; Chervy, T.; Zhang, L.; Thomas, A.; George, J.; Genet, C.; Hutchison, J. A.; Ebbesen, T. W. Energy Transfer between Spatially Separated Entangled Molecules. *Angew. Chem., Int. Ed.* **2017**, *56* (31), 9034−9038.
(36) Garcia-Vidal, F. J.; Feist, J. Long-Distance Operator for Energy Transfer. *Science* **2017**, *357* (6358), 1357−1358.
(37) Galego, J.; Garcia-Vidal, F. J.; Feist, J. Cavity-Induced Modifications of Molecular Structure in the Strong-Coupling Regime. *Phys. Rev. X* **2015**, *5* (4), 041022.
(38) Vasa, P.; Wang, W.; Pomraenke, R.; Lammers, M.; Maiuri, M.; Manzoni, C.; Cerullo, G.; Lienau, C. Real-Time Observation of Ultrafast Rabi Oscillations between Excitons and Plasmons in Metal Nanostructures with J-Aggregates. *Nat. Photonics* **2013**, *7* (2), 128−132.

DOI: 10.1021/acsphotonics.9b01357
ACS Photonics 2020, 7, 43−48